



HAL
open science

Silver-Tungsten induced codeposition: Influence of pH and carboxylic acid form in a DMH-based electrolyte

Quentin Orecchioni, Marie-Pierre Gigandet, Anna Krystianiak, Joffrey Tardelli, Jean-Yves Hihn

► **To cite this version:**

Quentin Orecchioni, Marie-Pierre Gigandet, Anna Krystianiak, Joffrey Tardelli, Jean-Yves Hihn. Silver-Tungsten induced codeposition: Influence of pH and carboxylic acid form in a DMH-based electrolyte. *Electrochimica Acta*, 2025, 509, pp.145335. 10.1016/j.electacta.2024.145335 . hal-04785365

HAL Id: hal-04785365

<https://hal.science/hal-04785365v1>

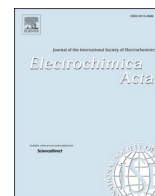
Submitted on 16 Nov 2024

HAL is a multi-disciplinary open access archive for the deposit and dissemination of scientific research documents, whether they are published or not. The documents may come from teaching and research institutions in France or abroad, or from public or private research centers.

L'archive ouverte pluridisciplinaire **HAL**, est destinée au dépôt et à la diffusion de documents scientifiques de niveau recherche, publiés ou non, émanant des établissements d'enseignement et de recherche français ou étrangers, des laboratoires publics ou privés.



Distributed under a Creative Commons Attribution 4.0 International License



Silver-Tungsten induced codeposition: Influence of pH and carboxylic acid form in a DMH-based electrolyte

Quentin Orecchioni^{a,b}, Marie-Pierre Gigandet^a, Anna Krystianiak^c, Joffrey Tardelli^b, Jean-Yves Hihn^{a,b,*}

^a Université de Franche-Comté, CNRS UTINAM UMR 6213 F-25030 Besançon, France

^b IRT M2P, F-57070 Metz, France

^c ICB UMR 6303 Université de Bourgogne, CNRS F-21078 Dijon, France

ARTICLE INFO

Keywords:

Silver-tungsten
Electrodeposition
Induced codeposition
DMH electrolyte

ABSTRACT

Silver-tungsten coatings were successfully electrodeposited on platinum and copper substrates from a non-toxic 5.5-dimethylhydantoin electrolyte at low pH and two different carboxylic acid forms: citrate or tartrate. Tungsten contents remain at low levels compared to former works, but close to the values considered as optimal for functional properties without having to recourse to controversial substances such as thiourea. Electrochemical studies by linear sweep voltammetry allow to distinguish two typical behaviors and give interesting insight into the induced codeposition mechanism. Silver-tungsten codeposition only occurred at pH 2.0 and 3.5 using citrates and at pH 2.0 using tartrates, corresponding to the forms H_3Cit , H_2Cit^{-2} , and H_2Tar , respectively. No silver-tungsten reduction was possible with less than two protonated carboxyl groups on either tartrate or citrate ions. Separate silver and tungsten lattice are both present in the resulting alloy. Grain and crystallite sizes were observed by SEM. XPS investigations show that for our low W content alloys, silver is found to be metallic whereas tungsten is present in oxide form. The carbon peaks and also gaps between peaks when N is absent indicate that citrates are present in the coating, unlike DMH.

1. Introduction

The connector industry is currently facing a strong demand for higher performance coatings, induced by various novel applications ranging from windmills to electric vehicles. Use of high voltages, associated with strong currents and connector coupling (more frequent insertion/removal), creates a strong demand for new properties, and silver alloys constitute interesting candidates for such a role.

In fact, pure silver exhibits the highest electrical conductivity among all metals [1,2]. Alloying silver with another element allows the coating to remain highly conductive due to a sufficient amount of silver, while the alloying element increases alloy performances (wear resistance, hardness, tarnishing). While innovative alloys with cobalt [3] and antimony [4] showed interesting properties, both metals are highly carcinogenic and thus, in view of European legislation, not suitable for industrial development.

Tungsten exhibits exceptional mechanical and corrosion properties [5,6]. Recently, increased interest has been shown in silver-tungsten

alloys as connectors for electrical and electronic purposes. Manufacturing methods of Ag-W alloys include powder metallurgy [7, 8], physical vapor deposition [9], electroless plating [10] and electrodeposition [11–18]. Tungsten reduction is often described as induced codeposition, meaning that it only occurs when another element is deposited at the same time. While the exact mechanism of silver tungsten induced codeposition is not yet fully understood, some hypotheses have been made. Early studies on induced tungsten codeposition alongside iron group metals postulated an intermediate tungsten-oxide state on the cathode prior to reduction into metallic tungsten by hydrogen catalyzed by the inducing metal [19]. Research about Ni-Mo codeposition proposed a similar mechanism, with the notable difference being the exact nature of the oxide form. Authors suggested that the Mo oxide layer formed a mixed oxide layer with Ni ions, before being reduced by adsorbed hydrogen [20]. Although this study was conducted with molybdenum, it proved to be relevant here given the similarities between tungstate and molybdate behaviors. Studying the mechanism of induced codeposition of molybdenum, rhenium, and tungsten, Eliaz and

* Corresponding author.

E-mail address: jean-yves.hihn@univ-fcomte.fr (J.-Y. Hihn).

<https://doi.org/10.1016/j.electacta.2024.145335>

Received 23 August 2024; Received in revised form 6 November 2024; Accepted 7 November 2024

Available online 8 November 2024

0013-4686/© 2024 The Author(s). Published by Elsevier Ltd. This is an open access article under the CC BY license (<http://creativecommons.org/licenses/by/4.0/>).

Gileadi suggest that the reaction implies the formation of a bimetallic complex. Considering previous work on Mo induced codeposition in Ni-Mo alloys [21] and publications about bi-metallic complexations [22, 23], Podlaha's group studied silver-tungsten induced codeposition from thiourea – citrate electrolytes at low pH [11], proposed an overall reaction and suggested that pH plays an important role during the formation of the adsorbed bimetallic complex. Aside from thiourea, there are occurrences of silver tungsten codeposition from ammonia-based electrolytes [16,24].

Various complexing agents were proposed as replacements for cyanide in silver plating, such as thiosulfate [25], sulfite [26], acetate [27], thiourea [28], ammonia [29], EDTA and derivatives [30], 2-hydroxypyridine [31], uracil [32], hydantoin and derivatives [33]. Among those, thiourea seems very promising, however its toxicity and carcinogenicity prevents its widespread use [34]. Therefore, nitrogen containing cyclic compounds especially 5,5-dimethylhydantoin [35–38], appears to be the most promising solutions. Their low toxicity [39] allow their use at industrial scale, particularly in Europe because “this product does not contain any substances listed in the candidate list of substances of very high concern at a concentration ≥ 0.1 % (EC regulation no 1907/2006 “REACH”, section 59)”. In fact 5,5-Dimethylhydantoin exhibits a stronger ability to form complexes with metal ions than other hydantoins [40]. Investigations on these complexes and their application in silver plating process suggested that one silver ion is chelated by two DMH molecules [41]. Silver alloys also witnessed the recent development of cyanide-free electrolytes [42–44]. Nevertheless, it is also necessary to take into account increasingly severe regulations, as well as an increased consideration of the need to protect operators. New formulations will need to allow for these aspects, eliminating the use of cyanides and avoiding controversial substances such as thiourea as much as possible.

In this paper, silver-tungsten induced codeposition is reported from a non-toxic DMH-based electrolyte at low pH on both platinum and copper. The resulting coatings were characterized by a variety of techniques. Electrochemical investigations, as well as change in pH and composition of the electrolyte, provide a better understanding of the mechanisms involved in the reaction.

2. Materials and methods

Solutions were prepared using the following salts: AgNO₃ cryst. extrapure Merck, Ag₂SO₄ ≥ 99 % PanReac, 5,5-dimethylhydantoin ≥ 97 % Sigma-Aldrich, Na₂WO₄·2H₂O ≥ 97 % Roth, C₆H₅Na₃O₇·2H₂O sodium citrate ≥ 99 % Roth, C₄H₄Na₂O₆·2H₂O Sodium L-(+)-tartrate ≥ 99 % Alfa Aesar. All salts were weighed on a precision scale before being mixed and dissolved in deionized water. Solutions were then adjusted to the selected pH via addition of concentrated KOH or H₂SO₄. pH was measured using a Mettler-Toledo pH-meter. Electrolytes were left for 1 hour under mechanical stirring before use.

Voltametric experiments were conducted in a 20 mL three-electrode cell equipped with a rotating disk electrode (RDE) as working electrode. Measurements were taken using a Biologic SP-240 potentiostat. The reference electrode was an Orygalys Hg/Hg₂Cl₂ combined with a salt bridge filled with saturated K₂SO₄ to avoid chloride ions in the silver electrolyte. A pure platinum wire was used as counter electrode. The working electrode was a Radiometer rotating disk electrode with a 2 mm diameter platinum tip. Before each experiment the RDE tip was cleaned with concentrated nitric acid before being polished on polishing cloth using 1 μ m diamond suspension.

Deposits were elaborated on a platinum disk by applying the chronoamperometric mode with constant potential for a fixed charge quantity of 100 mC in the mentioned 20 mL three-electrode cell. No stirring was applied during deposition. The tip was then rinsed with deionized water and ethanol before being dried with hot air.

X-Ray Fluorescence (XRF) measurements of coating thickness and composition were carried out using a Fischer X-Ray XDV-SDD

instrument with a dedicated method calibrated on pure elements. Measurement time was set to 30 s.

Dynamic viscosity of the solution was evaluated using the Kinexus rheometer by Malvern in shear stress mode averaged on three measurements.

Coatings were made on a 1 \times 1 cm copper substrate. Sample preparation included surface degreasing with ethanol, activation in a 3.7 %_w HCl solution, and presilvering before proceeding to actual silvering. The presilvering step was conducted in a three-electrode configuration in a 40 mL beaker under stirring. The presilvering electrolyte was composed of 0.05 M AgNO₃ and 0.15 M 5,5-dimethylhydantoin at pH 13.0. This layer was deposited in chronoamperometric mode at a constant -0.30 V/SCE potential for 30 s. Aside from preventing displacement reduction on less noble copper, this layer avoids changes in reduction potentials as the future reaction will occur directly on the silver surface. After presilvering, the sample was coated in the silver-tungsten plating bath. The deposition was conducted in a 40 mL beaker, 3-electrodes setup, in chronoamperometric mode at a chosen constant potential defined by the voltammetry curves. The coating on copper plate was made under agitation, with a relatively high concentration of silver compared to other academic studies (but closer to industrial bath ones) which limits the effects of mass transport. Therefore, all electrodeposits have been elaborated at a controlled potential, and current densities were equivalent to the one observed with RDE on Pt, meaning very close agitation conditions.

For cross-section observation of silver-tungsten coatings on copper substrate, the sample was cut in half before being cold-mounted in an epoxy resin. The sample was mirror-polished using diamond suspension before observation.

Scanning electron microscope (SEM) observations were made using a Tescan MIRA3 FEG SEM. The Sam-X EDS Module was used to conduct measurements at 30 keV tension.

X-Ray Diffraction (XRD) experiments were conducted on a Bruker D8 Discover instrument using a copper tube in μ XRD mode via a 1 mm collimator. Scans ranged from 20 to 100° for 2 θ values with an increment of 0.02° and a speed of 1 second per step.

The elemental surface composition of coatings and precipitate products were measured by X-ray Photoelectron Spectroscopy (XPS). Spectra were obtained using an XPS-Auger PHI 5000 VersaProbe (Physical Electronics, Minnesota, USA) equipped with a monochromatic Al K α X-ray source ($h\nu = 1486.6$ eV) operated at 50 W (15 kV, 3.3 mA). Measurements were performed in ultra-high vacuum (10^{-7} / 10^{-8} Pa). The analytical area of analysis is a disc 200 μ m in diameter. Spectra were collected at a take-off angle of 45°.

3. Results and discussion

3.1. Silver-tungsten codeposition from DMH—Citrate electrolyte at low pH

The ratios between the different bath components were similar to those determined by Podlaha's group in their pioneering work on silver-tungsten [11], but avoiding the use of thiourea that is replaced mostly by 5,5-dimethylhydantoin. The electrolyte was composed of 0.05 M AgNO₃, 0.15 M DMH, 0.2 M Na₂WO₄·2H₂O, and 0.2 M Na₃C₆H₅O₇·2H₂O. Even if DMH is documented for silver plating under alkaline conditions, experiments were conducted at pH 2, recreating similar conditions to those presented in the paper.

Voltammeteries were first conducted without any agitation at varying scan rates, ranging from 2 to 50 mV s⁻¹. Resulting voltammograms are presented in Fig. 1(a).

The voltammograms show two strong reduction peaks. By conducting voltammetry between the addition of each component, the peak at +0.3 V/SCE was identified as the silver reduction peak and the peak below -0.6 V/SCE is attributed to current limitation due to tungsten oxide precipitation, induced by the pH increase by the proton

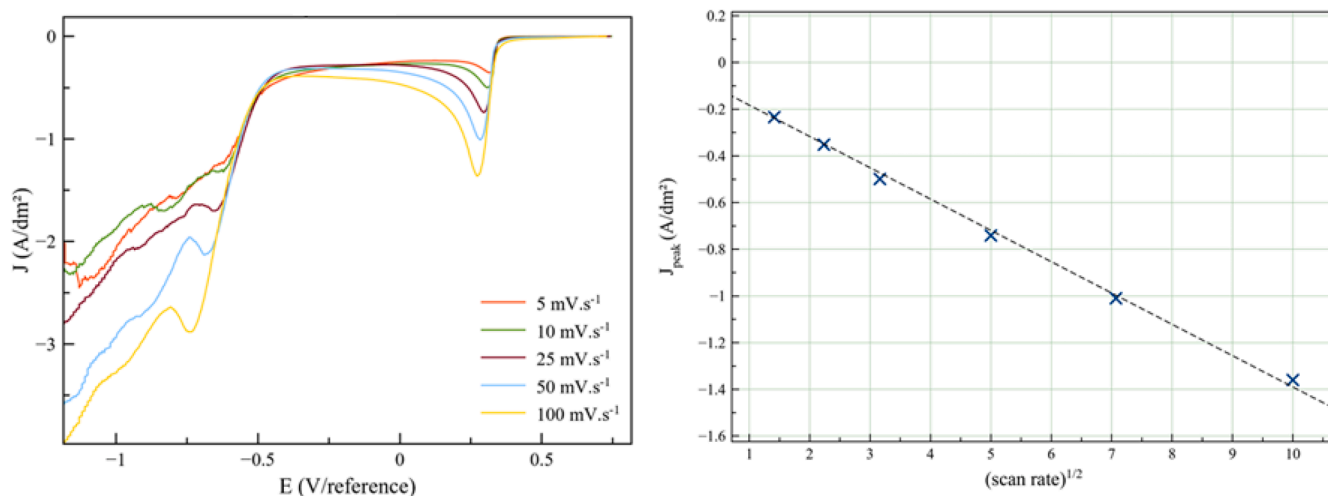


Fig. 1. (a) voltammograms of the citrate-DMH electrolyte at pH=2.0 and varying scan rates (b) intensity of the silver peak (+0.3 V/SCE) versus square root of the scan rate.

consumption during the electrolysis. Moving continuously to more negative potential, the solvent reduction is strong enough to overcome this barrier. A deposition on platinum RDE was conducted as described in the experimental section at +0.28 V/SCE. The resulting deposit was characterized by XRF. The coating was 3.24 μm , while the tungsten content was 2.5 %wt. Experiments on platinum RDE were also conducted in an electrolyte using Ag_2SO_4 instead of AgNO_3 as a silver source, but keeping the same metal concentration in the bath. The voltammograms are identical to those obtained with silver nitrate in the same conditions. A silver-tungsten layer was electrodeposited on RDE following the same protocol, and the values of thickness and tungsten content are similar to those of the previous sample, at 3.10 μm and 2.2 %wt, respectively. Considering the higher cost of Ag_2SO_4 and the absence of significant change in the electrochemical behavior of the electrolyte, unless when clearly specified, all the other experiments in this study were conducted using AgNO_3 as a silver source.

However, the voltammograms did not show dissociated peaks for silver or tungsten reduction. By varying the scan rate, reduction peak intensity increases. Peak intensity is proportional to the square root of the scan rate, as shown in Fig. 1(b), meaning that this reaction is limited

by diffusion.

Voltametric experiments were then conducted at a fixed 2 $\text{mV}\cdot\text{s}^{-1}$ scan rate, to remain in a steady state at each point, but with varying rotation speeds ranging from 200 to 600 rpm. The voltammograms obtained are shown in Fig. 2.

By using the Levich equation (Equation 1), the diffusion coefficient can be calculated from plateau intensity and rotation speed at various potentials. This was calculated using three different potentials: +0.165V/SCE, +0.175V/SCE, and +0.185V/SCE.

$$I_{lim} = 0.62 \times n \times F \times D_i^{2/3} \times \omega^{1/2} \times \nu^{-1/6} \times C_i^*$$

Equation 1: Levich equation used to calculate the diffusion coefficient of the silver complex in the DMH-citrate electrolyte.

Dynamic viscosity of the solution was measured using a rheometer, while density was calculated by weighing 20 mL of the plating bath into a volumetric flask. Kinematic viscosity of the plating bath was evaluated at $3.088 \times 10^{-6} \text{ m}^2 \text{ s}^{-1}$. Considering the low tungsten content in the coating, we chose to consider only silver ions for further calculations. The diffusion coefficient, which is related to the nature of the complexed silver ions, was determined to be $8.92 \times 10^{-6} \text{ cm}^2 \text{ s}^{-1}$. This value is lower

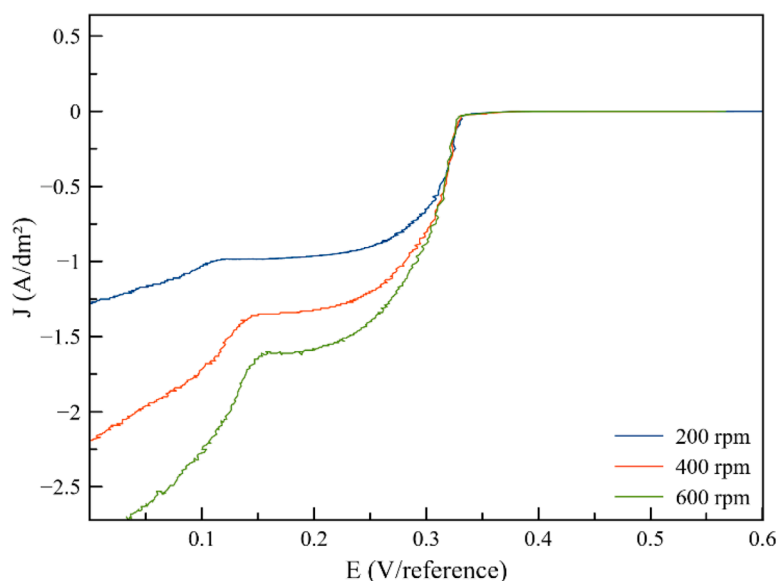


Fig. 2. Voltammograms of the DMH-Citrate electrolyte at pH 2.0; 2 mV/s and varying rotation rates of the RDE.

than diluted silver nitrate [45] and higher than other silver complexes [46], while staying within the same order of magnitude. Diffusion coefficient deviating from diluted AgNO_3 toward complexed silver values, even with small amplitude, indicate that silver may be chelated by 5,5-dimethylhydantoin and/or citrate ions.

Then, a deposit was conducted on a 1 cm^2 copper plate following the protocol described in the experimental section at $+0.28 \text{ V/SCE}$, which corresponds to the silver reduction peak. Coating thickness and composition were measured by XRF and averaged on 16 measurements. The resulting electrodeposited Ag-W layer composition was $2.84 \%_{\text{wt}}$ in tungsten and $5.61 \mu\text{m}$ thick. To be used as a reference for comparison in microstructures studies, a second plating bath was composed exactly as described above, but without tungstate ions. From this modified electrolyte, a pure silver coating was electrodeposited on the bare copper substrate.

To pursue further investigations, the samples were cut in half and prepared as described in the experimental section before SEM imaging, XPS, EDS and XRD analysis. EDS analysis on the sample cross-section showed a tungsten content of $2.94 \%_{\text{wt}}$ averaged on 3 measurements, thus confirming the values obtained previously by XRF. Thickness was evaluated by SEM at $6.27 \mu\text{m}$ on three points of the Ag-W coating, slightly higher than the $5.61 \mu\text{m}$ measured by XRF. A possible explanation for this gap is that the SEM observation was very narrow, whereas the XRF measurements covered the entire surface of the sample. The SEM observations are presented in Fig. 3. For the silver coated sample,

visible grain size is between 2.5 and $3 \mu\text{m}$ (Fig. 3(a)), while crystallite size is between 15 and 20 nm (Fig. 3(b)) which is comparable to what is obtained from cyanide electrolyte [47] but with a completely different morphology. The incorporation of tungsten in the coating does not influence the microstructure (Fig. 3(d)) and only a small decrease of the grain size could be noted (Fig. 3(c)). Except for thickness, no significant information was obtained from cross-section observations.

XRD analyses were then conducted on bare copper substrate, on silver-coated sample, and on silver-tungsten coated sample. Diffractograms are shown in Fig. 4.

From the substrate, we distinguish a series of peaks related to copper at the following values of 2θ : 43° , 45° , 50° , 74° , 90° , and 95° . The pure silver sample shows two contributions: a face-centered cubic (FCC) with a lattice parameter of 0.408 nm , which is standard for silver [48], and another FCC with a lattice parameter of 0.430 nm . This can be attributed to the insertion of another element in the silver lattice. Concerning the Ag-W coated sample, the two contributions of silver are still visible. A new peak is visible at $2\theta = 57.5^\circ$, which could be associated with a tungsten body-centered lattice with a parameter of 0.139 nm . The electrodeposited silver-tungsten layer is constituted of separate phases of silver and tungsten. However, the presence of tungsten insertion in the silver lattice cannot be affirmed or refuted without further investigations. A strong orientation along the (022) plan is visible in the deposit.

XPS analyses were conducted on Ag and Ag-W coated copper sample.

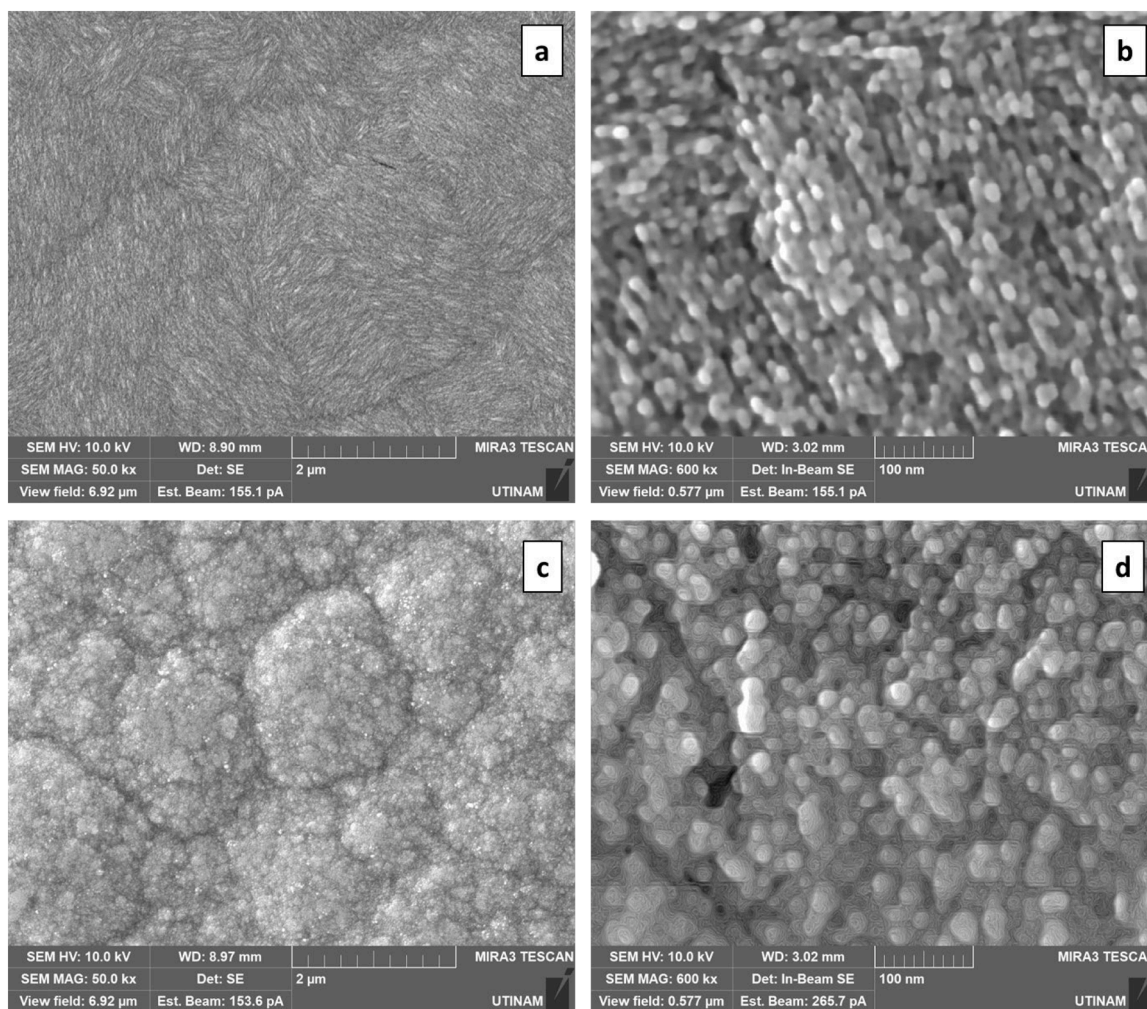


Fig. 3. SEM observations of pure Ag and Ag-W coating on copper substrate at various magnifications (a) x50k micrograph of pure silver coating (b) x600k micrograph of pure silver coating (c) x50k visible grain structure of silver tungsten coating (d) x600k with visible crystallites of silver tungsten coating. All coatings were elaborated at $\text{pH}=2.0$.

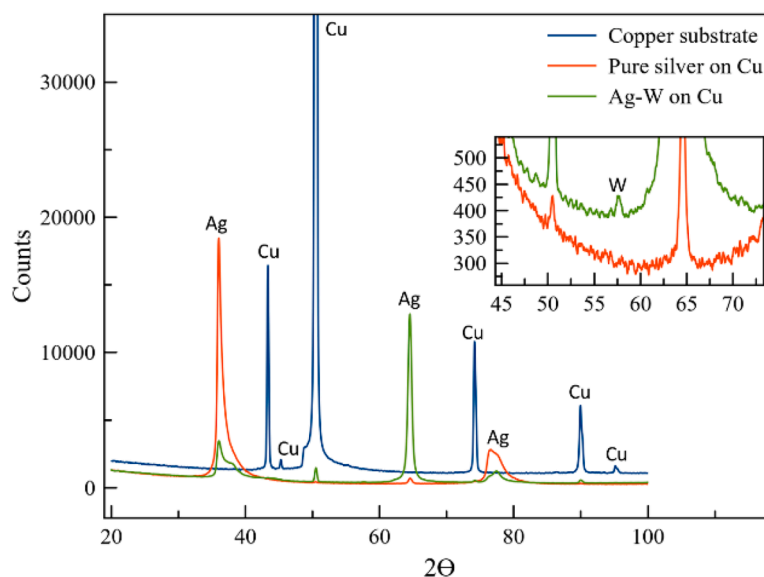


Fig. 4. Diffractograms obtained from the copper substrate, silver-coated substrate, and silver-tungsten coated copper.

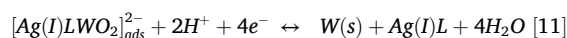
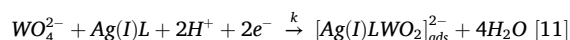
Silver was found to be metallic in all cases with no oxide nor sulfur compounds (Fig. 5(a)). Considering the tungsten, only oxide-related peaks were visible on spectra (Fig. 5(b)). This is not in accordance with XRD diffractogram showing a peak associated with metallic tungsten (Fig. 4). But not abnormal considering the tendency of W to form passivation layer and the weak analysis depth of XPS (6nm). However, even with over 10 nm etching, no metallic tungsten was put in evidence. Following our investigations on of C and N inclusions into the deposits. C was found bounded to C—C/C—H (pollution), and to C—O, C=O and O—C=O (Fig. 5(c)). Not only the peak presence, but also the regularity of the gaps between peaks, is the typical signature of citrates. Moreover, it was shown that N was nearly absent whatever the conditions, confirming the absence of DMH in the deposit.

Silver-tungsten codeposition on platinum and copper was successfully conducted from DMH-citrate bath at low pH. However, if silver was found to be reduced in a metallic nanocrystalline state, the tungsten chemical form is not obvious.

Tungstate reduction needing not less than six electrons and eight protons, is very unlikely to happen in a single step. Two possible explanations proposed in the literature may be discussed for the DMH—Citrate electrolyte.

Some authors explained induced codeposition by the formation of a bimetallic adsorbed complex [12]. The first step is the partial reduction of tungstate ions in an adsorbed bimetallic compound which is further reduced in another step. Complexed silver ions are spectators in this reaction. This theory has been reported for various couples of inducing and induced element including silver-tungsten [11]. It should be noted that this was observed with silver-tungsten obtained from

Thiourea-citrate electrolyte reaching much higher W content in the deposit than the present work. The codeposition reaction could be described as the following equation, where L represents the ligand:



Equation 2: Overall reaction of tungsten induced codeposition with silver. k indicates that the first step is limited by kinetic.

Another possible mechanism is the formation of a solid oxide on the electrode before its reduction to metal by the presence of adsorbed hydrogen. This was proposed for the deposition of W together with Fe, Co and Ni as the inducing element [19]. A partially reduced tungstate film is deposited before being catalytically reduced by hydrogen in the presence of the inducing element. A similar explanation was provided in the case of Ni-Mo alloy deposition, where an electrodeposited Mo oxide reacts with Ni²⁺ to form a mixed Ni-Mo oxide, which is then reduced to Ni-Mo by hydrogen under strong polarization [20]. This could also apply to W alloys due to the close behaviors of tungstate and molybdate ions.

The XPS results obtained here are well-suited to the theory of an intermediate oxide formation since W_xO_y compounds were detected. The absence of Ag-O peaks suggests that in our case, no other mixed oxide is formed on the cathode. The process remains jammed at the oxide stage because there is little or no competition with HER (hydrogen discharge) under the deposition conditions used. Therefore, no hydrogen is adsorbed and available to reduce the mentioned oxide into metallic tungsten, which leads to the absence of metallic tungsten.

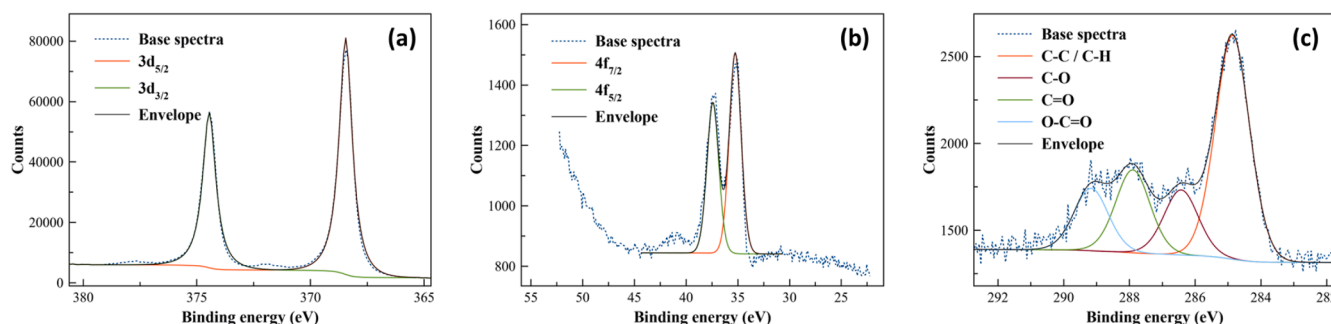


Fig. 5. XPS spectra of Ag-W coating on Cu. (a) Silver related peaks (b) Tungsten related peaks (c) Carbon related peaks.

At this point, it is difficult to be conclusive, especially if one takes into account the possible detection of metallic tungsten by XRD, which would be in contradiction with the XPS measurements, and taking into account that the latter are always difficult in the case of highly reactive metals with a strong tendency to natural oxidation. This may suggest the coexistence of different mechanisms in silver-tungsten codeposition. A similar occurrence of W and W_xO_y simultaneous deposition was reported in the literature concerning Zn-W alloy codeposition [49]. Authors suggested that the mechanism behind W reduction involves multiple steps, sometime leading to only partial reduction and codeposition of tungsten oxides.

Eventually in both cases, surface supply is more challenging for silver complex ions than for tungstate ones, and it is possible to assume that silver reduction is under mass transport control while tungsten reduction is under kinetic control. In the case of the bimetallic complex, its formation occurs only at the electrode surface. According to equation 2 [11], WO_4^{2-} and complexed silver are reduced in the first step of the overall mechanism. Therefore, the bimetallic complex is not expected to be present in bulk solution but formed at the surface after adsorption. This implies that only the silver complex is limited by mass transport as shown by voltammograms of Fig. 2, where silver diffusion is related to RDE rotation rates. If the main route is reduction of tungstate ions into oxide directly on the surface, the limitation by diffusion is probably the same and concerns only silver complexed ions. Therefore, as silver is less concentrate, and much more present in the coating, the surface supply in silver complexed ions is more difficult. This is evidenced too by the limitation of silver transport (Levich). On the contrary, tungsten consumption is so low that its supply is not limited by mass transport. This is comforted by the independence of W concentration in the deposit, independent of the W concentration in the bulk solution.

3.2. pH influence on silver-tungsten induced codeposition

In their work on silver-tungsten induced codeposition, Podlaha's group mentioned that pH plays a prominent role in the reaction [11]. The influence of the form of the complexing agents was evaluated by conducting experiments at various pH. As tartrate ions are mentioned in a XTalic patent concerning cyanide-free silver-tungsten plating [50], they were used in the present work as a comparison with citrate ions to better understand the role of the carboxyl groups.

3.2.1. pH influence on DMH-citrate electrolyte

As presented in the first part, silver-tungsten electrodeposition was conducted under acidic conditions in a DMH-Citrate electrolyte. However, use of DMH in silver plating is mainly documented at high pH values [35,37,38], when the molecule is in its deprotonated form [51]. Considering the various possible forms of citrate depending on media

acidity [52], at least 6 pH values of interest can be defined. The forms of DMH and citrate at each pH are shown in Table 1, alongside the main associated citrate-tungsten complexes in solution [53]. In total, eight possible forms of citrate tungstate complexes are present in solution in variable amount, but, for clarity purpose, only the predominant ones are mentioned in the table. Silver is most likely complexed as $[Ag(DMH)_2]^+$ at higher pH [41], $[Ag_3(C_6H_5O_7)_{n+1}]^{3n-}$ in more neutral media [54] while it may also exist as free Ag^+ under acidic conditions. However, interactions between citrate, DMH, tungstate and silver remain unknown and therefore, no statement could be made on the exact nature of complexes in solution.

Experiments were conducted on six different electrolytes, all using the same composition described in the first part of the paper, but with pH adjusted to different values. For each electrolyte, voltammetry was performed at $25 \text{ mV}\cdot\text{s}^{-1}$. The voltammograms are presented in Fig. 6. Electrodepositions were conducted on platinum at various potentials in each electrolyte following the protocol described in the experimental section. The coated RDE was then characterized by XRF after deposition.

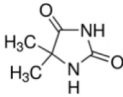
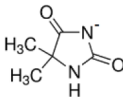
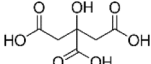
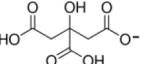
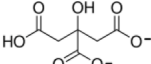

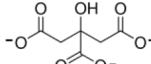

A distinct change in electrochemical behavior of the solution is observed between pH=5.0 and pH=8.0. The "acidic" behavior, for pH lower than 5.0, shows only two peaks: one associated with silver and tungsten around +0.3 V/SCE, and one associated with tungstate precipitation below -0.5 V/SCE. The "alkaline" behavior, for pH higher than 8.0, shows several low intensity peaks for at least 3 different reactions. The peak at -1.0 V/SCE may be linked to tungsten-species precipitation due to local pH variation. In view of such variation of voltammograms depending on the pH of the electrolyte, citrate forms seem to have a great influence on bath electrochemistry.

Deposits were made on platinum RDE at various potentials for each pH and analyzed by XRF to detect presence or absence of tungsten in the coating. For pH 2.0 and 3.5, tungsten was detected at 2.50 and 1.65 %_w, respectively (averaged on 5 measurements). Pursuing investigations, one copper sample was silver-tungsten coated at pH 3.5 and characterized as described in the first part of this work. The resulting coating was similar to the one obtained at pH=2 both on morphology and crystallinity. For pH 5.0, 8.0, 9.19, and 13.0, only pure silver was electro-deposited regardless of deposition potential. Considering the change in tungsten content between pH 2.0 and 3.5 and the fact that no tungsten was deposited at pH 5.0, the citrate form seems to play a prominent role in the induced tungsten reduction. According to these observations and applying it to Equation 2, Citrate-silver complexes may play the role of Ag(I)L in the DMH-Citrate electrolyte.

Without being a key factor for tungsten reduction, DMH forms greatly influence electrolyte stability. In fact, plating bath behavior differs significantly depending on the pH. Pictures of the solutions were taken 5 days after preparation under stirring and are shown in Fig. 7. At pH 5.0 and 8.0, the solution forms a large amount of white precipitate

Table 1

Citrate and DMH predominant species depending on solution pH. Citrate ion pKa are 3.13, 4.76, and 6.40. DMH pKa value is 9.19. Dissociation constant of the tungsten-citrate complexes are $10^{21.67}$, $10^{17.03}$ and $10^{10.2}$ for $[WO_4CitH_3]^{2-}$, $[WO_4CitH_2]^{3-}$, and $[WO_4CitH]^{4-}$ respectively [53].

pH	2.0	3.5	5.0	8.0	9.19	13.0
DMH form			DMH		Equimolar ratio of protonated and deprotonated form	[DMH] ⁻
						
Citrate form	H ₃ Cit	H ₂ Cit ⁻	HCit ²⁻		Cit ³⁻	
Major tungsten form in solution	 [WO ₄ CitH ₃] ²⁻	 [WO ₄ CitH ₂] ³⁻	 [WO ₄ CitH] ⁴⁻	 [WO ₄ CitH] ⁴⁻	 WO ₄ ²⁻ + [WO ₄ CitH] ⁴⁻	 WO ₄ ²⁻

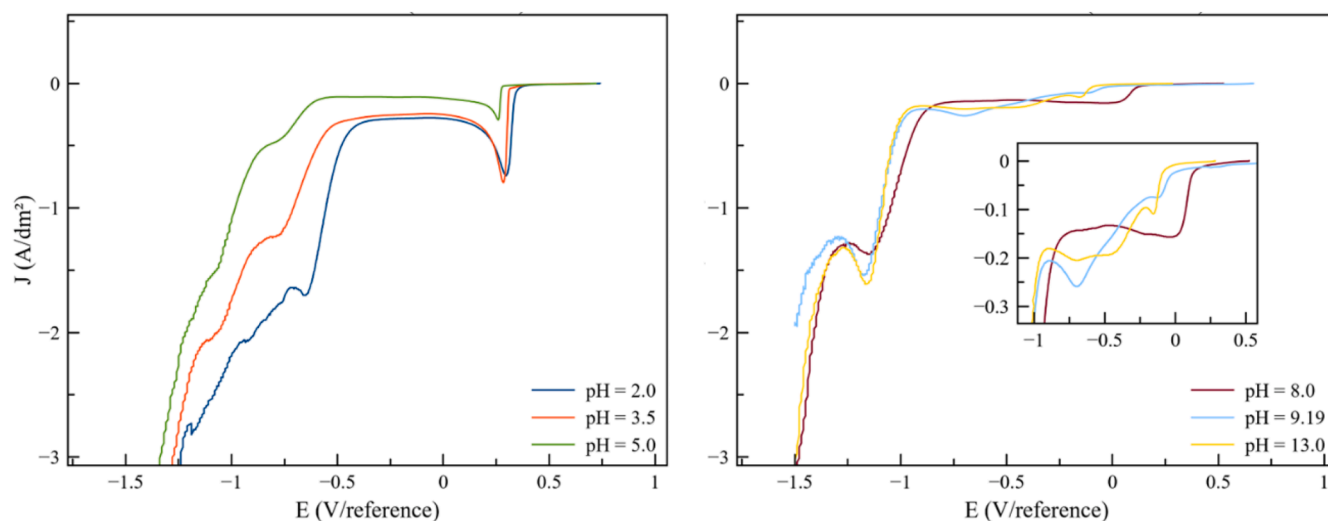


Fig. 6. Voltammograms obtained at $25 \text{ mV}\cdot\text{s}^{-1}$ at various pH in the DMH-citrate electrolyte. On the left, (a) the "acidic" behavior and on the right, (b) the "alkaline" behavior.

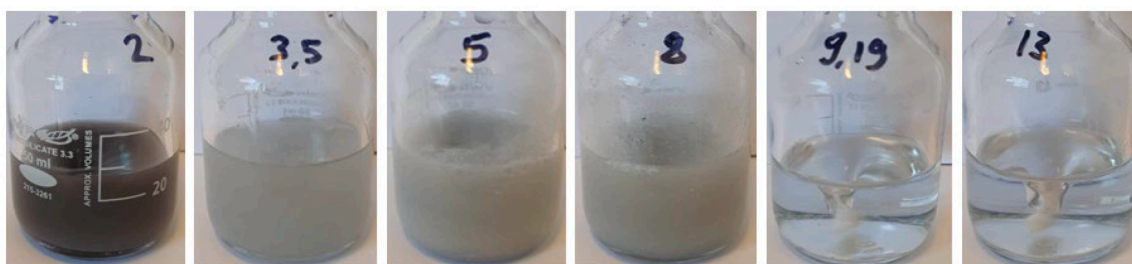


Fig. 7. DMH—Citrate electrolyte at various pH under stirring 5 days after preparation. From left to right, (a) pH 2.0, (b) pH 3.5, (c) pH 5.0, (d) pH 8.0, (e) pH 9.19, and (f) pH 13.0.

instantly after preparation. At pH 2.0 and 3.5, the solution is slightly turbid after preparation and precipitates within 72 h. However, precipitate nature differs between the two: at pH 2.0, the precipitate is brown to black, very similar to what can be observed with silver nitrate solutions alone, while at pH 3.5, the precipitate is light gray, closer to what is observed at pH 5.0 and 8.0. Electrolytes prepared at higher pH show a clear colorless appearance and a great stability, due to the ability of DMH to form complexes with silver under alkaline conditions. At pH higher than 9.19, DMH-silver complexes are strong enough to prevent precipitation of AgCl when adding a drop of saturated KCl in the solution, which is not the case for all the other pH values.

The same 6 solutions were prepared without DMH and precipitated instantly, regardless of the pH. 5.5-dimethylhydantoin is therefore the main factor in electrolyte stability, even at low pH.

An experiment was carried out using Ag_2SO_4 instead of AgNO_3 as a silver source at pH 2.0. A picture of this solution after 5 days under stirring is shown in Fig. 8(a). Just as with nitrate, the solution was turbid after preparation but remained in this state and showed no black precipitate after 5 days. The precipitated solutions were Buchner filtered, and the dried precipitates were analyzed by X-ray photoelectron spectroscopy. As insufficient solid was recovered from the solution at pH 3.5, characterizations were conducted only on pH 2.0, 5.0, and 8.0. Precipitation products were found to be very similar in the solutions at pH 5.0 and 8.0. Without identifying the exact chemical nature of those precipitates, XPS results allow for some discrimination between samples. For example, nitrogen content was higher at pH 5.0 and 8.0 compared to pH 2.0, while not being related to nitrate bond, therefore meaning that those precipitates contain DMH. Silver was found in similar quantities regardless of solution pH. At pH 2.0, tungsten content is significantly

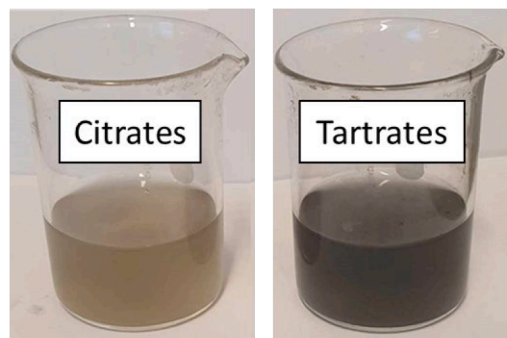


Fig. 8. Electrolyte prepared with Ag_2SO_4 as a silver source under stirring 5 days after preparation. (a) on the left, DMH—Citrate electrolyte, (b) on the right, DMH—Tartrate electrolyte.

higher than in the other samples. Formation of solid tungstic acid at low pH described in the literature can offer a possible explanation for this difference [55]. The exact cause of precipitation of those electrolytes remains unknown but could be the subject of future investigations.

Moreover, some solutions are photosensitive, regardless of silver sources (silver sulfate, silver methanesulfonate, silver nitrate have been tested) and to the complexation strength. This must be taken into account, as electrolyte stability is a serious issue for practical applications.

3.2.2. pH influence on DMH-Tartrate electrolyte

Experiments were conducted using tartrate ions instead of citrate in the electrolyte. Whereas citric acid presents three carboxyl groups,

tartaric acid has only two. To compensate for this and maintain the same concentration of carboxyl groups in the solution, tartrate concentration was raised from 0.2 to 0.3 M. The electrolyte is therefore composed of 0.05 M AgNO_3 , 0.15 M DMH, 0.2 M $\text{Na}_2\text{WO}_4 \cdot 2\text{H}_2\text{O}$, and 0.3 M $\text{Na}_2\text{C}_4\text{H}_4\text{O}_6 \cdot 2\text{H}_2\text{O}$. Considering the various forms of tartrate ions and their related pKa [56], four electrolytes were investigated. For each of them, solution acidity was chosen to promote one predominant form of tartrate ions. Solution pH was adjusted to 2.0, 3.7, and 6.0 corresponding to H_2Tar , HTar , and Tar^{2-} , respectively, as the predominant species. Another solution was prepared at pH 13.0 to evaluate the influence of the DMH form.

Concerning solution stability, pH 2.0 showed a dark violet coloration along with the formation of black precipitate, similar to what was observed with citrate. The difference is that the formation of this precipitate occurred within the first 24 h after preparation. The solution at pH 3.7 was turbid after preparation and witnessed the formation of light gray precipitate over three days, whereas the solution at pH 6.0 precipitated instantly after preparation. The solution at pH 13 remained clear and colorless after 5 days. An experiment was carried out using Ag_2SO_4 as a silver source. Contrary to citrate, the solution containing tartrate ions and silver sulfate turned black after 5 days. Pictures of the two solutions are shown in Fig. 8. These observations could mean that tartrate ions are detrimental to solution stability compared to citrates.

For each electrolyte, voltammetry was carried out at $25 \text{ mV} \cdot \text{s}^{-1}$, and depositions on platinum were conducted at different potentials according to the protocol described in the experimental section. An analysis was then conducted by XRF to determine the presence or absence of tungsten in the deposit. Resulting voltammograms are presented in Fig. 9. The curve for pH 6.0 was represented by a black dotted line as intensity was very low, due to the formation of large quantities of silver hydroxide precipitate.

Similarly to what was observed with citrate ions, both electrochemical behavior changes between pH 3.7 and pH 6.0. Samples with pH below 3.7 show a strong reduction peak around $+0.3 \text{ V/SCE}$, which is absent for higher pH values. Silver-tungsten codeposition was achieved but only at pH 2.0, while all other depositions on platinum resulted in pure silver deposit. Considering these results alongside what was obtained with citrate ions, silver-tungsten induced codeposition occurred only when the carboxylic acid predominant form showed at least two protonated carboxyl groups, whether they were H_3Cit , H_2Cit^- or H_2Tar . Silver-tungsten codeposition is reported with citrate at pH 3.5

but not with tartrate at pH 3.7 indicating that, in the same pH range, the codeposition occurred only in presence of double protonated ligand suggesting that regardless of the pH the protonation state of the chelating agent may be the mandatory factor. An overall recap of the electrochemical observations is shown in Fig. 10.

4. Conclusion

Silver-tungsten coatings were successfully electrodeposited from a non-toxic DMH-citrate electrolyte at low pH on both platinum rotating disk electrodes and copper plates. Tungsten contents remain at low levels compared to former works, but close to the values considered as optimal for functional properties (wear resistance increase while maintaining low resistivity). Moreover, DMH-citrate electrolyte appears as a sustainable alternative, without having to recourse to controversial substances such as thiourea, and therefore avoiding sulfur incorporation.

The diffusion coefficient of complexed silver ions in the electrolyte was calculated using the Levich equation. This value will help further investigations on the complex in future works. Separate silver and tungsten lattice are both present in the resulting alloy. Grain and crystallite sizes were observed by SEM on silver and silver-tungsten coated copper samples. While XRD results showed presence of metallic tungsten in the coating, only tungsten oxide species were detected in XPS investigations. Some interesting comparisons are possible with former works on tungsten and molybdenum codeposition mechanisms involving the creation of an intermediate oxide layer on the cathode.

While this work gave interesting insight of the tungsten induced codeposition with silver, the mechanism will need further studies to be fully understood. Indeed, the point is the reduction of WO_4^{2-} at the interface. Results on using citrate and tartrate ions as a function of pH, for tungsten induced codeposition with silver in DMH-based electrolyte allow to better understand the role of the carboxyl groups on the reaction, following a behavior coherent with Podlaha's model i.e. formation of an intermediate bimetallic complex. Silver-tungsten codeposition only occurred at pH 2.0 and 3.5 using citrates and at pH 2.0 using tartrates, corresponding to the forms H_3Cit , $\text{H}_2\text{Cit}^{2-}$, and H_2Tar , respectively. It was found that absence or presence of tungsten in the deposit was not linked to the shape of the voltammograms. In fact, the prominent factor in the tungsten induced reduction seems to be the protonation state of the carboxylic acid used in the electrolyte. No silver-

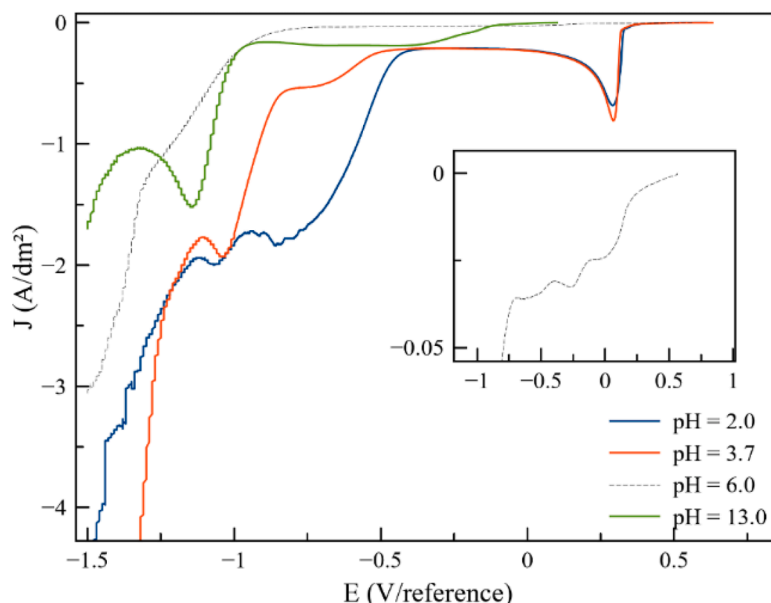


Fig. 9. Voltammograms obtained at $25 \text{ mV} \cdot \text{s}^{-1}$ and various pH in the DMH-Tartrate electrolyte.

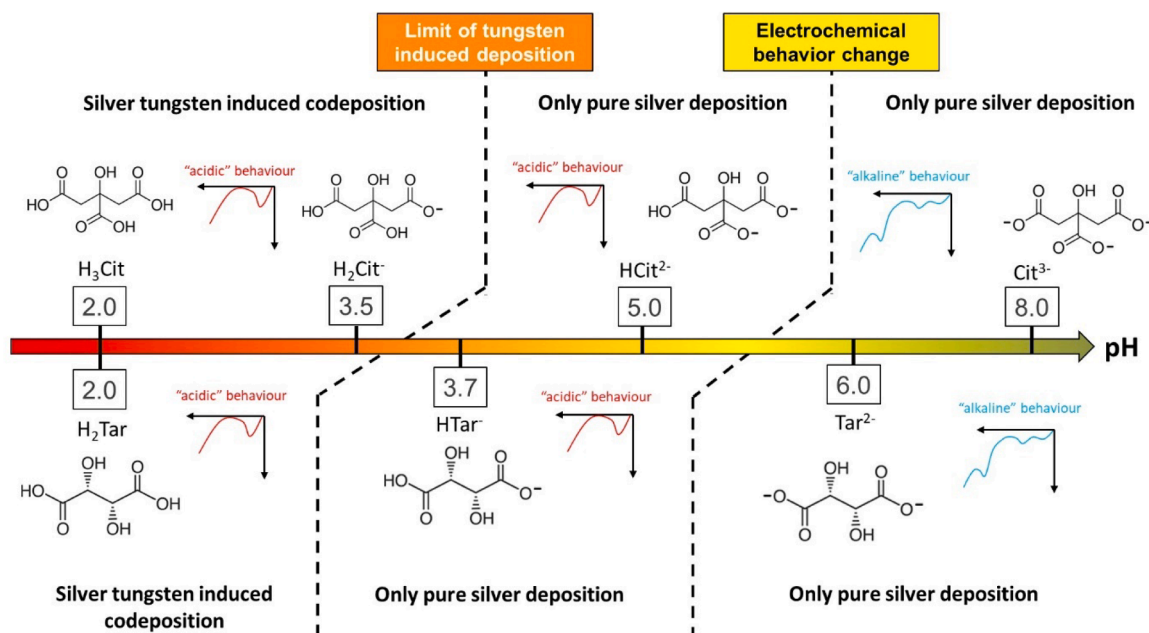


Fig. 10. Overall recap of the behavior of the electrolyte depending on the pH and nature of the carboxylic acid used.

tungsten reduction was possible with less than two protonated carboxyl groups on either tartrate or citrate ions.

Nevertheless, the predominance of tungsten oxide in the deposit draws attention to the coexistence of several steps before obtaining pure metallic tungsten. These observations must be seen in context of low tungsten content in the coating and relative absence of hydrogen discharge that does not allow to achieve a more complete reduction.

While not being the main factor influencing the electrochemical behavior of the electrolyte, 5,5-dimethylhydantoin plays a major role in stabilization. However, the DMH—Citrate plating bath does not seem ideal for silver-tungsten reduction as this reaction only occurs at low pH values when the electrolyte is not stable for more than 72 h.

CRediT authorship contribution statement

Quentin Orecchioni: Writing – original draft, Investigation, Conceptualization. **Marie-Pierre Gigandet:** Methodology, Investigation. **Anna Krystianiak:** Investigation. **Joffrey Tardelli:** Validation, Methodology, Funding acquisition. **Jean-Yves Hihn:** Writing – original draft, Supervision, Methodology, Conceptualization.

Declaration of competing interest

The authors declare the following financial interests/personal relationships which may be considered as potential competing interests:

Jean-Yves HIHN reports financial support was provided by IRT M2P. Olivier Heintz reports equipment, drugs, or supplies was provided by PIA-excellence ISITE-BFC. If there are other authors, they declare that they have no known competing financial interests or personal relationships that could have appeared to influence the work reported in this paper.

Acknowledgements

The authors would like to express their acknowledgements to the IRT M2P Metz for its financial support (SILAHPERF project). The authors also thank the UTINAM chemistry platform PCU and especially Mr. Nicolas ROUGE for his precious help (SEM/EDS analysis), Ms. Virginie MOUTARLIER for her precious advice and time for XRD characterizations. Thanks is due to the ARCEM—Carnot platform (ICB) and especially

to Mr. Olivier HEINTZ for his assistance in XPS analysis, supported by the PIA-excellence ISITE-BFC (COMICS project “Chemistry of Molecular Interactions Catalysis and Sensors” FEDER).

Data availability

Data will be made available on request.

References

- [1] M. Myers, Overview of the Use of Silver in Connector Applications (503-1016), (n. d.) 14.
- [2] D.R. Smith, F.R. Fickett, Low-temperature properties of silver, J. Res. Natl. Inst. Stand. Technol. 100 (1995) 119, <https://doi.org/10.6028/jres.100.012>.
- [3] S. Nineva, T.S. Dobrovol'ska, I. Krastev, Properties of electrodeposited silver–cobalt coatings, J. Appl. Electrochem. 41 (2011) 1397–1406, <https://doi.org/10.1007/s10800-011-0361-5>.
- [4] V.I. Balakai, A.V. Arzumanova, A.V. Starunov, I.V. Balakai, Properties of electrolytic silver-based alloy, Inorg. Mater. Appl. Res. 9 (2018) 947–953, <https://doi.org/10.1134/S2075113318050027>.
- [5] S.B. Lyon, Corrosion of tungsten and its alloys. Shreir's Corrosion, Elsevier, 2010, pp. 2151–2156, <https://doi.org/10.1016/B978-0-44452787-5.00105-0>.
- [6] E. Pink, R. Eck, Refractory metals and their alloys, in: R.W. Cahn, P. Haasen, E. J. Kramer (Eds.), Materials Science and Technology, 1st ed., Wiley, 2006 <https://doi.org/10.1002/9783527603978.mst0088>.
- [7] M.T. Kesim, H. Yu, Y. Sun, M. Aindow, S.P. Alpay, Corrosion, oxidation, erosion and performance of Ag/W-based circuit breaker contacts: a review, Corros. Sci. 135 (2018) 12–34, <https://doi.org/10.1016/j.corsci.2018.02.010>.
- [8] F. Findik, H. Uzun, Microstructure, hardness and electrical properties of silver-based refractory contact materials, Mater. Des. 24 (2003) 489–492, [https://doi.org/10.1016/S0261-3069\(03\)00125-0](https://doi.org/10.1016/S0261-3069(03)00125-0).
- [9] A. Kaidatzis, V. Psycharis, D. Niarchos, Sputtered tungsten–silver and tungsten–aluminum thin films for non-volatile magnetic memories applications, Microelectron. Eng. 159 (2016) 6–8, <https://doi.org/10.1016/j.mee.2016.01.021>.
- [10] V. Bogush, A. Inberg, N. Croitoru, V. Dubin, Y. Shacham-Diamand, Electroless deposition of novel Ag–W thin films, Microelectron. Eng. 70 (2003) 489–494, [https://doi.org/10.1016/S0167-9317\(03\)00414-3](https://doi.org/10.1016/S0167-9317(03)00414-3).
- [11] A. Kola, X. Geng, E.J. Podlaha, Ag–W electrodeposits with high W content from thiourea–citrate electrolytes, J. Electroanal. Chem. 761 (2016) 125–130, <https://doi.org/10.1016/j.jelechem.2015.12.002>.
- [12] N. Eliaz, E. Gileadi, Induced codeposition of alloys of tungsten, molybdenum and rhenium with transition metals, in: C.G. Vayenas, R.E. White, M.E. Gamboa-Aldeco (Eds.), Modern Aspects of Electrochemistry, Springer New York, New York, NY, 2008, pp. 191–301, https://doi.org/10.1007/978-0-387-49489-0_4.
- [13] Z.B. Jiao, C.A. Schuh, Nanocrystalline Ag–W alloys lose stability upon solute desegregation from grain boundaries, Acta Mater. 161 (2018) 194–206, <https://doi.org/10.1016/j.actamat.2018.09.014>.
- [14] K. Bui, T. Hasanali, T. Goodrich, New final finish stack including a custom nanocrystalline silver alloy for mobile connector systems with high cycling wear and

- powered environmental exposure requirements, in: 2015 IEEE 65th Electronic Components and Technology Conference (ECTC), IEEE, San Diego, CA, 2015, pp. 1907–1913, <https://doi.org/10.1109/ECTC.2015.7159861>.
- [15] T. Goodrich, K. Bui, A. Athans, J. Cahalen, M. Osborne, P. Stokoe, Performance testing and evaluation of a Ag-W nano-crystalline silver alloy as a gold replacement in electrical connectors, in: 2014 IEEE 60th Holm Conference on Electrical Contacts (Holm), IEEE, New Orleans, LA, USA, 2014, pp. 1–7, <https://doi.org/10.1109/HOLM.2014.7031051>.
- [16] N. Dadvand, M. Dadvand, Pulse electrodeposition of nanostructured silver-tungsten-cobalt oxide composite from a non-cyanide plating bath, *J. Electrochem. Soc.* 161 (2014) D730–D735, <https://doi.org/10.1149/2.0371414jes>.
- [17] D. Höhlich, T. Mehner, I. Scharf, T. Lampke, Simultaneous electrodeposition of silver and tungsten from [EMIm]Cl:AlCl₃ ionic liquids outside the glove box, *Coatings* 10 (2020) 553, <https://doi.org/10.3390/coatings10060553>.
- [18] P. Bacal, P. Indyka, Z. Stojek, M. Donten, Unusual example of induced codeposition of tungsten. Galvanic formation of Cu–W alloy, *Electrochem. Commun.* 54 (2015) 28–31, <https://doi.org/10.1016/j.elecom.2015.02.016>.
- [19] W.E. Clark, M.H. Lietzke, The mechanism of the tungsten alloy plating process, *J. Electrochem. Soc.* 99 (1952) 245, <https://doi.org/10.1149/1.2779712>.
- [20] E. Chassaing, K. Vu Quang, R. Wiart, Mechanism of nickel-molybdenum alloy electrodeposition in citrate electrolytes, *J. Appl. Electrochem.* 19 (1989) 839–844, <https://doi.org/10.1007/BF01007931>.
- [21] E.J. Podlaha, D. Landolt, Induced Codeposition: I. An Experimental Investigation of Ni-Mo Alloys, *J. Electrochem. Soc.* 143 (1996) 885–892, <https://doi.org/10.1149/1.1836553>.
- [22] O. Younes, E. Gileadi, Electroplating of Ni/W Alloys, *J. Electrochem. Soc.* (2024) 12, n.d.
- [23] O. Younes-Metzler, L. Zhu, E. Gileadi, The anomalous codeposition of tungsten in the presence of nickel, *Electrochim. Acta* 48 (2003) 2551–2562, [https://doi.org/10.1016/S0013-4686\(03\)00297-4](https://doi.org/10.1016/S0013-4686(03)00297-4).
- [24] N.V. Bogush, A.A. Khmyl, L.K. Kushner, N.V. Dezhkunov, Composition, structure and functional properties of silver-tungsten composition electrochemistry coatings formed with the help of ultrasound, *Doklady Belorusskogo Gosudarstvennogo Universiteta Informatiki i Radioelektroniki* 19 (2021) 23–31, <https://doi.org/10.35596/1729-7648-2021-19-6-23-31>.
- [25] F. Ren, L. Yin, S. Wang, A.A. Volinsky, B. Tian, Cyanide-free silver electroplating process in thiosulfate bath and microstructure analysis of Ag coatings, *Trans. Nonferrous Metals Soc. China* 23 (2013) 3822–3828, [https://doi.org/10.1016/S1003-6326\(13\)62935-0](https://doi.org/10.1016/S1003-6326(13)62935-0).
- [26] A. Valiūnienė, G. Baltrūnas, R. Valiūnas, G. Popkirov, Investigation of the electroreduction of silver sulfite complexes by means of electrochemical FFT impedance spectroscopy, *J. Hazard. Mater.* 180 (2010) 259–263, <https://doi.org/10.1016/j.jhazmat.2010.04.023>.
- [27] Y.-H. Wang, C.-C. Liao, C.-H. Kuo, X.-H. Huang, S.-T. Chen, C.-H. Wu, Y.-H. Hsueh, S.-F. Ou, Controlled aggregation of Ag nanoparticles on oxide templates on nitinol by electrodeposition, *Mater. Lett.* 267 (2020) 127531, <https://doi.org/10.1016/j.matlet.2020.127531>.
- [28] B. Reents, W. Plieth, V.A. Macagno, G.I. Lacconi, Influence of thiourea on silver deposition: spectroscopic investigation, *J. Electroanal. Chem.* 453 (1998) 121–127, [https://doi.org/10.1016/S0022-0728\(98\)00217-4](https://doi.org/10.1016/S0022-0728(98)00217-4).
- [29] M. Miranda-Hernández, I. González, Effect of potential on the early stages of nucleation and growth during silver electrocrystallization in ammonium medium on vitreous carbon, *J. Electrochem. Soc.* 151 (2004) C220, <https://doi.org/10.1149/1.1646154>.
- [30] G.M. De Oliveira, M.R. Silva, I.A. Carlos, Voltammetric and chronoamperometric studies of silver electrodeposition from a bath containing HEDTA, *J. Mater. Sci.* 42 (2007) 10164–10172, <https://doi.org/10.1007/s10853-007-2102-z>.
- [31] Z.-B. Lin, J.-H. Tian, B.-G. Xie, Y.-A. Tang, J.-J. Sun, G.-N. Chen, B. Ren, B.-W. Mao, Z.-Q. Tian, Electrochemical and In Situ SERS Studies on the Adsorption of 2-Hydroxypyridine and Polyethyleneimine during Silver Electroplating, *J. Phys. Chem. C* 113 (2009) 9224–9229, <https://doi.org/10.1021/jp909761f>.
- [32] B.-G. Xie, J.-J. Sun, Z.-B. Lin, G.-N. Chen, Electrodeposition of mirror-bright silver in cyanide-free bath containing uracil as complexing agent without a separate strike plating process, *J. Electrochem. Soc.* 156 (2009) D79, <https://doi.org/10.1149/1.3046157>.
- [33] A. Liu, X. Ren, J. Zhang, D. Li, M. An, Complexing agent study for environmentally friendly silver electrodeposition(ii): electrochemical behavior of silver complex, *RSC Adv.* 6 (2016) 7348–7355, <https://doi.org/10.1039/C5RA23766A>.
- [34] Safety Data Sheet Sigma-Aldrich Thiourea CAS n° 66-56-6, (n.d.).
- [35] Z. Hajiahmadi, Z. Tavangar, Proposing a new complexing agent for cyanide-free silver electroplating through a comprehensive computational study of dimethyl hydantoin, *Mol. Simul.* 47 (2021) 619–627, <https://doi.org/10.1080/08927022.2021.1895436>.
- [36] F. Pizzetti, E. Salvietti, W. Giurlani, R. Emanuele, C. Fontanesi, M. Innocenti, Cyanide-free silver electrodeposition with polyethyleneimine and 5,5-dimethylhydantoin as organic additives for an environmentally friendly formulation, *J. Electroanal. Chem.* 911 (2022) 116196, <https://doi.org/10.1016/j.jelechem.2022.116196>.
- [37] A. Liu, X. Ren, J. Zhang, G. Yuan, P. Yang, J. Zhang, M. An, A composite additive used for an excellent new cyanide-free silver plating bath, *New J. Chem.* 39 (2015) 2409–2412, <https://doi.org/10.1039/C4NJ02060J>.
- [38] A. Liu, X. Ren, C. Wang, J. Zhang, C. Du, R. Han, M. An, DMH and NA-based cyanide-free silver electroplating bath: a promising alternative to cyanide ones in microelectronics, *Ionics (Kiel)* 27 (2021) 417–422, <https://doi.org/10.1007/s11581-020-03541-5>.
- [39] Safety Data Sheet Sigma-Aldrich 5,5 Dimethylhydantoin CAS n° 77-71-4, (n.d.).
- [40] G.Z. Pavlovich, R.G. Luthy, Complexation of metals with hydantoins, *Water Res.* 22 (1988) 327–336, [https://doi.org/10.1016/S0043-1354\(88\)90160-1](https://doi.org/10.1016/S0043-1354(88)90160-1).
- [41] A. Liu, X. Ren, M. An, J. Zhang, P. Yang, B. Wang, Y. Zhu, C. Wang, A combined theoretical and experimental study for silver electroplating, *Sci. Rep.* 4 (2014) 3837, <https://doi.org/10.1038/srep03837>.
- [42] Y. Sun, G. Zangari, Phase Separation in Electrodeposited Ag-Pd Alloy Films from Acidic Nitrate Bath, *J. Electrochem. Soc.* 166 (2019) D339–D349, <https://doi.org/10.1149/2.1231908jes>.
- [43] D. Liang, W. Shao, G. Zangari, Selection of Phase Formation in Electroplated Ag-Cu Alloys, *J. Electrochem. Soc.* 163 (2016) D40–D48, <https://doi.org/10.1149/2.0651602jes>.
- [44] R. Bernasconi, J.L. Hart, A.C. Lang, L. Magagnin, L. Nobili, M.L. Taheri, Structural properties of electrodeposited Cu-Ag alloys, *Electrochim. Acta* 251 (2017) 475–481, <https://doi.org/10.1016/j.electacta.2017.08.097>.
- [45] J.G. Firth, H.J.V. Tyrrell, Diffusion Coefficients for Aqueous Silver Nitrate Solutions at 25°, 35°, and 45° from Diaphragm-cell Measurements, *J. Chem. Soc.* (1962) 2042–2047.
- [46] S. Vandeputte, B. Tribollet, A. Hubin, J. Vereecken, Electrohydrodynamic impedance investigation of silver electrode position in a thiosulphate ligand system, *Electrochim. Acta* 39 (1994) 2729–2741, [https://doi.org/10.1016/0013-4686\(94\)E0191-2](https://doi.org/10.1016/0013-4686(94)E0191-2).
- [47] A. Nevers, L. Hallez, F. Touyeras, J.-Y. Hihn, Effect of ultrasound on silver electrodeposition: crystalline structure modification, *Ultrason. Sonochem.* 40 (2018) 60–71, <https://doi.org/10.1016/j.ultrsonch.2017.02.033>.
- [48] I. Krstev, M. Nikolova, Structure of silver electrodeposits plated from different complex electrolytes, *J. Appl. Electrochem.* 16 (1986) 703–706, <https://doi.org/10.1007/BF01006922>.
- [49] H. Kazimierczak, N. Eliaz, Induced codeposition of tungsten with zinc from aqueous citrate electrolytes, *Coatings* 13 (2023) 2001, <https://doi.org/10.3390/coatings13122001>.
- [50] N. Dadvand, C.A. Schuh, A.C. Lund, J.C. Trenkle, J. Cahalen, Coated articles and methods, US 8,936,857 B2, n.d.
- [51] G. Kortum, W. Vogel, K. Andrussov, Dissociation constants of organic acids in aqueous solution, (1961).
- [52] S. Rode, C. Henninot, C. Vallières, M. Matlosz, Complexation chemistry in copper plating from citrate baths, *J. Electrochem. Soc.* 151 (2004) C405, <https://doi.org/10.1149/1.1715092>.
- [53] J.J. Cruywagen, L. Kruger, E. Rohwer, Complexation of Tungsten(vi) with Citrate, *J. Chem. Soc. Dalton Trans.* (1991).
- [54] S. Djokić, Synthesis and antimicrobial activity of silver citrate complexes, *Bioinorg. Chem. Appl.* 2008 (2008) 436458, <https://doi.org/10.1155/2008/436458>.
- [55] T. Barre, L. Arurault, F. Sauvage, Chemical behavior of tungstate solutions. Part 1. A spectroscopic survey of the species involved, *Spectrochimica Acta Part A* 61 (2005) 551–557, [https://doi.org/10.1016/S1386-1425\(04\)00248-3](https://doi.org/10.1016/S1386-1425(04)00248-3).
- [56] R.M.C. Dawson, D.C. Elliott, *Data For Biochemical Research*, Clarendon Press, Oxford, 2002, 3. ed., repr.